Precise Navigation on Soft Tissues with an Endomicroscopy Probe

Benoît Rosa*†, Jérôme Szewczyk*, Guillaume Morel*
*Institute of Intelligent Systems and Robotics, UPMC - University Pierre et Marie Curie, CNRS - UMR 7222, Paris, France
†Department of Mechanical Engineering, KU Leuven

***Abstract*—Probe-based Confocal Laser Endomicroscopy (pCLE) is a recent image modality that could allow to perform optical biopsies, without taking a tissue sample. This is of particular interest in laparoscopy, to diagnose and grade cancer in the abdominal cavity.**

Among the different problems that arise when trying to take optical biopsies inside the abdominal cavity, the control of the probe motion is of upmost importance. Indeed, it is not only necessary to stabilize the images on the organs, but also to move the probe along the tissue surface to reconstruct large field of view images needed by pathologists. This can be done using a mosaicking algorithm.

This paper presents a visual servo control scheme for controlling the probe navigation on the tissue. Its robustness is challenged in an *ex vivo* setup using a high-accuracy industrial robot. The achieved precision is good enough to allow for reconstructing large field of images with controlled shape and size, and high resolution.

I. Introduction

In oncology, biopsy is a standard procedure that aims at determining the cancer nature and development stage of a suspected tissue. It consists in taking a tissue sample out of the patient in order to analyze it under a microscope. Anatomopathologists usually analyze the cells themselves but also their relative organization from a larger picture to make their diagnosis. Prior to this, they need to prepare the tissue for microscope examination. Usually, the tissue is frozen or fixed using paraffin and cut in thin slices of a few microns, then stained using special markers that highlight cellular structures (for instance, hematoxylin-eosin staining which is used un clinical routine).

In digestive surgery, extemporaneous biopsies can be carried out, i.e. biopsies made during the operating time. In that case, the surgeon takes the tissue sample, sends it to the anatomopathologist, and waits for his/her answer that will orient the following of the procedure. For instance, in the event of a tumor resection, the surgeon must be sure that the resection margins are free of tumour cells. The time that the pathologist spends preparating the tissue is then just a waiting time during which the patient is under global anesthesia. Moreover, taking a tissue sample is invasive, which limits the number of biopsies that can be done on a same organ. This is particularly problematic for staging laparoscopies, in which the surgeon explores the abdominal cavity and needs to take several biopsies in order to find metastases and properly grade the cancer development stage [1], [2].

To circumvent those limitations, it has been proposed to take "optical biopsies", i.e. without taking a tissue sample. The surgeon then needs to bring an image modality, here a microscope, *in situ* in order to take images that can directly be transmitted to the surgeon. Different image modalities can be used, for instance OCT [3] and confocal endomicroscopy (pCLE) [4], [5]. In this paper, we focus on confocal endomicroscopy. This image modality works with fluorescence imaging, which is interesting because functional imaging can be realized by using the proper fluorescent agent. This image modality is currently used in clinical practice during endoluminal examinations, for instance for diagnosis of Barrett's esophagus [6], [7]. It tipycally has a resolution of one micron, and a field of view of 200x240 microns. The images are acquired at a 12 Hz rate.

Several problems arise when trying to use pCLE in endoscopic examinations. First, contrarily to endoluminal examinations, the flexible probe is not in a tube. Therefore, organ motions must be taken into account. In the abdominal cavity, organs move in a range of a few centimeters each second due mainly to breathing and persitaltis. This particular problem has been the subject of many research, and solved either using passive [8] or force-controlled [9] stabilization. Second, the field of view in the pCLE images is usually too narrow for the pathologist to analyze the cellular structures properly. It has been reported previously that pathologists need a $1-3\ mm^2$ field of view, whereas a single image is only $0.04\ mm^2$. The same problem had already been reported in endoluminal examinations, and mosaicking algorithms have been developped in order to enhance the field of view [10], [11]. The principle is to move the probe along the tissue – while staying in contact, which is needed for acquiring images – and to register images together in order to reconstruct a large field of view image. Moving the probe inside a laparoscopic instrument can be done using specific microactuators [8], [12], but it has been shown in [13] that even with a very precise control of the probe motion, tissue deformations prevent from making high quality mosaics.

In this paper, we present a visual servoing approach that allows to control the probe trajectory on the tissue with microscopic precision.

This work was supported by OSEO (Maisons-Alfort, France) under ISI Project PERSEE (number I0911038W) and by French state funds managed by the ANR within the Investissements d'Avenir programme (Labex CAMI) under reference ANR-11-LABX-0004

II. Endomicroscopy-based visual servoing

This section presents the visual servoing scheme that is used for controlling the probe motion. First, a quick look at the mosaicking algorithm from [10] helps to understand image metrics and scan requirements, then the visual servoing control loop is presented.

A. Notations

In the following, V refers to speeds whereas X refers to positions. They both are vectors. Subscripts $_r$, $_p$, $_a$ and $_0$ refer to the robot holding the probe, the probe, the anatomical tissue and a fixed base, respectively. For instance, $V_{p/a}$ denotes the relative velocity between the probe and the anatomical tissue.

B. Mosaicking algorithm

The mosaicking algoithm used in this work was published in [10]. The main part of the problem is reconstructing the trajectory that has been followed in the images. This is done in two steps (see fig. 1).

First, successive images are registered together (real-time mosaicking, fig. 1a) using normalized cross-correlation [14]. This computation is made in one pass with a Fourier transform, so it has a fixed computational budget and is suited for real-time. This allows to compute an estimation $\widehat{V}_{p/a}$ of $V_{p/a}$, and therefore to estimate $X_{p/a}$ by simply integrating it (eq. 1).

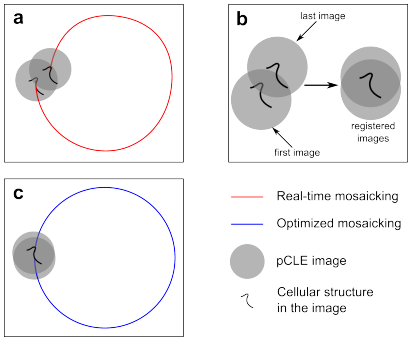

Figure 1. General principle of the mosaicking algorithm. a: real-time mosaicking; b: registration of spatially but not temporally closed images; c: optimized mosaicking.

$$\widehat{X}_{p/a}(t) = \widehat{X}_{p/a}(0) + \int_0^t \widehat{V}_{p/a}(\tau)d\tau \tag{1}$$

The problem of registering successive images together to sum the registration results, as in eq. 1, is that the total error at the end of the trajectory is the sum of each registration error. It can be seen in fig. 1a that cellular structures are not properly aligned due to this cumulative error. The second part of the mosaicking algorithm is meant to eliminate this drift. By analyzing the real-time mosaicking trajectory, one can find images that are spatially close but not temporally close. Registering those images together (fig. 1b) and then performing an optimization scheme (fig. 1c) leads to an enhanced mosaic. This is particularly important, because mosaic images reconstruction leads to blurred and duplicate structures in the images if cumulative errors are not taken into account.

C. Scanning requirements

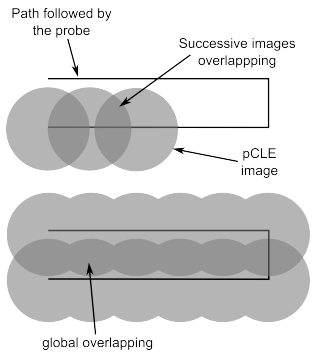

Figure 2. Scanning requirements in terms of overlapping

Scanning a tissue in order to make a mosaic needs specific requirements (see fig. 2). First, sucessive images should overlap of approximately 80% to obtain good results with open-loop mosaicking. This leads to a scanning speed on the tissue of approximately 0.3 mm/s or less. 0.3 mm/s is preferred because a lower speed means a larger scanning time.

Second, overlap between scan lines (global overlap) must be sufficient to compute mosaics (50-100 microns overlap between scanning lines). To make a 3 mm^2 mosaic, a raster scan trajectory of 15 straight parallel lines of 1500 microns length is proposed. It has been shown in [15] that drift in the real-time mosaicking is low enough to allow for computing optimized mosaics if such a trajectory can be followed with approximately 50 microns precision.

D. Position-based visual servoing (PBVS)

It has been shown in [13] that tissue deformations play an important role when scanning at the contact of the tissue. Therefore, we propose here to use the measurements of the real-time mosaicking algorithm to control the probe motion.

The setup that we have here is a robot r controlling the movements of a probe p relatively to a fixed base 0 in order to follow a trajectory on a tissue a. In other words, we want to compute the required speed $V_{r/0}$ so that the estimated image position $X_{p/a}$ follows a given scanning trajectory X_d. Usually, in visual servoing, a simple proportional controller ensures an exponential convergence of the error towards zero. Here, since the image velocity is not null, a feedforward term should be added. However, we have here additional disturbances with the tissue deformations. Exponential convergence of the error cannot be obtained with a simple proportional gain since probe motions don't necessary make the image move. Therefore, an additional integral gain is added. The resulting control loop then writes, with K_P and K_I being repsectively the proportional and integral gains:

$$\begin{aligned} V_{r/0} = \frac{\mathrm{d}X_d}{\mathrm{d}t} + K_P\left(X_d(t) - \widehat{X}_{p/a}(t)\right) + \\ K_I \int_0^t \left(X_d(\tau) - \widehat{X}_{p/a}(\tau)\right) d\tau \end{aligned} \tag{2}$$

III. Experimental setup and results

A. Experimental setup

The experimental setup is presented on fig. 3. The confocal imaging system is a Cellvizio with a UHD probe (Mauna Kea Technologies, France). The probe is fixed at the end effector of a TX40 robot (Stubli, Faverges, France), through a prototype probe holder. The robot has 6 Degrees of Freedom (DoF) and exhibits a 20 µm repeatability at its end effector. The tissue samples are put on a rough surface that is fixed with respect to the robot base and parallel to the horizontal plane. Considering the small size of the scanned areas (a few square millimeters), the scanned tissues are considered as planar in this study. Therefore, the robot movements are generated at a constant height z_0 . Meanwhile, the probe orientation is kept constant, which finally results in a 2 DoF planar positioning problem. The cartesian position of the optical head is controlled by the on-board controller of the TX40 robot which is interfaced for allowing real-time update. Tissues are stained with Acriflavine for fluorescence.

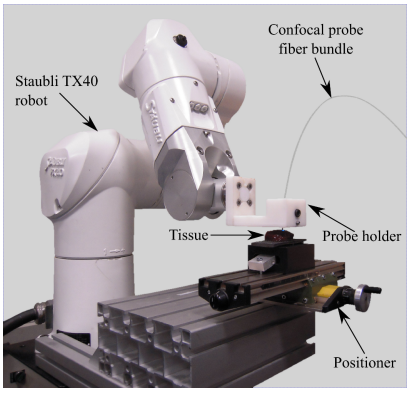

Figure 3. Experimental setup with a TX40 robot

B. Ex vivo experiments on soft tissues

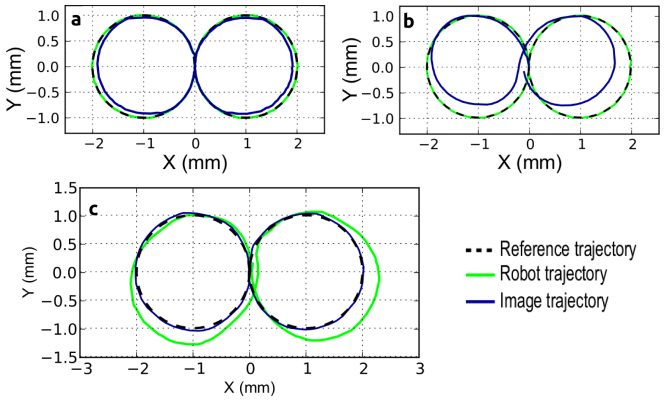

Figure 4. Data recorded during the performing of 8-shape trajectories. a: on a piece of paper glued to a rigid surface. b: on a piece of beef liver with open-loop control. c: on a piece of beef liver with closed-loop control.

1) Simple trajectory: On figure 4 can be seen the results of several scans with an 8-shape trajectory formed of two circles of 1 mm each. The results on paper (fig. 4a) clearly indicate that the robot control is very precise, according to its own measurements. A marginal error of 140 microns occurs at the farthest point of the trajectory, indicating a possible deformation of the probe holder or a robot modeling error. Most importantly, drift due to real-time mosaicking between first and last image is less than 10 microns, which has been observed in repeated experiments.

As expected, results on soft tissue (fig. 4b) show a very large shift relatively to the reference trajectory. The mean distance error between the image trajectory and the reference trajectory is more than 300 µm, and the final error is 150 µm. This shows that the tissue deformation has a direct and non negligible impact on the trajectory effectively followed by the probe relative to the tissue.

Finally, applying visual servoing allows to follow the reference trajectory with high accuracy (fig. 4c). The error between the first and the last image is 15 µm and the mean tracking position error is 30 µm. This improvement with respect to the open-loop results from fig. 4a and fig. 4b shows that the tissue and probe holder deformations are rejected by the visual control algorithm.

2) Large field of view mosaics: The next experiment is a mosaic obtained by servoing the image to follow the 3 mm^2 raster scan desired trajectory described previously. The two mosaics (real-time and optimized) are presented in fig. 5. The performance of the visual servo control allows to make sure that each line will overlap with the next one, thus making the computation of an optimized mosaic possible. This results in an optimized mosaic that has very low drift : the gain can be observed on fig. 5 when zooming to particular regions. The general shape of the optimized mosaic does not change with respect to the real-time mosaic, but blurred regions disappear. This gain in resolution is expected to make the analysis of the images by a pathologist easier.

IV. Conclusion

This paper presents a visual servo control scheme for navigating precisely on a soft tissue, for large field of view mosaicking purposes. A particular problem that has to be taken into account is the tissue deformation phenomenon, which is evidenced in the paper and acts as a disturbance to be rejected by the controller.

A simple PI closed loop control and a feedforward action is sufficient for rejecting unmodelled tissue deformations. The precision of the tracking allows for computing large mosaics with proper overlapping. Resulting mosaics are of good quality thanks to subsequent optimization of the images positions in the mosaic.

Future research will direct towards integrating the tissue model that has been proposed and validated in [13] in order to enhance the tracking performances of this visual servo control scheme. Integration in minimally invasive instruments for *in vivo* evaluation is also considered.

Acknowledgement

The authors thank their partners in the PERSEE project: Mauna Kea Technologies (project leader, Paris, France), Endocontrol Medical (Grenoble, France), Institut Mutualiste Montsouris (Paris, France) and Institut Gustave Roussy.

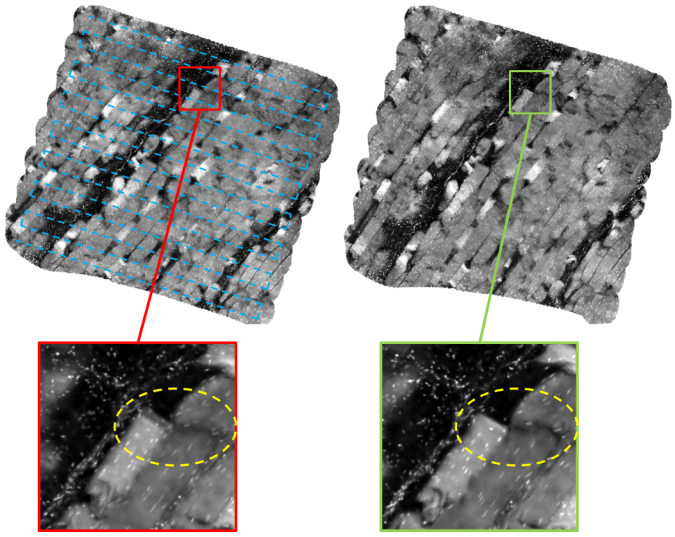

Figure 5. Square 1.7 x 1.7 mm raster scan mosaics constituted with 1600 images obtained under visual servoing (chicken breast). Left: real-time mosaic with the raster scan desired trajectory in dashed blue; right: optimized mosaic. Zooming on details show that, for the optimized mosaic, the precision of the off-line registration allowed by proper layer overlapping leads to see microscopic details with reduced blur, for example in the yellow dashed ellipse.

The project also largely benefits from the interaction with three anthropologists, Marie-Christine Pouchelle, Caroline Moricot and Marina Maestrutti, who are warmly thanked (support from CNRS, PE/PS program of INSHS and from INCA – the national institute of cancer).

REFERENCES

[1] Y. Hori, "Diagnostic laparoscopy guidelines," *Surgical Endoscopy*, vol. 22, no. 5, pp. 1353–1383, 2008.

[2] V. Muntean, A. Mihailov, C. Iancu, R. Toganel, O. Fabian, I. Domsa, and M. Muntean, "Staging laparoscopy in gastric cancer. accuracy and impact on therapy," *J. Gastrointestin. Liver Dis.*, vol. 18, no. 2, pp. 189–195, 2009.

[3] L. Hariri, G. Bonnema, K. Schmidt, A. Winkler, V. Korde, K. Hatch, J. Davis, M. Brewer, and J. Barton, "Laparoscopic optical coherence tomography imaging of human ovarian cancer," *Gynecologic oncology*, vol. 114, no. 2, pp. 188–194, 2009.

[4] G. L. Goualher, A. Perchant, M. Genet, B. Viellerobe, B. Abrat, and N. Ayache, "Towards optical biopsies with an integrated fibered confocal fluorescence microscope," in *Proc. IEEE International Conference on Medical Image Computing and Computer-Assisted Intervention (MICCAI'04)*, 2004, pp. 761–768.

[5] M. Wallace, P. Fockens *et al.*, "Probe-based confocal laser endomicroscopy." *Gastroenterology*, vol. 136, no. 5, p. 1509, 2009.

[6] R. Kiesslich, L. Gossner, M. Goetz, A. Dahlmann, M. Vieth, M. Stolte, A. Hoffman, M. Jung, B. Nafe, P. Galle *et al.*, "In vivo histology of barrett's esophagus and associated neoplasia by confocal laser endomicroscopy," *Clinical Gastroenterology and Hepatology*, vol. 4, no. 8, pp. 979–987, 2006.

[7] P. Sharma, A. Meining, E. Coron, C. Lightdale, H. Wolfsen, A. Bansal, M. Bajbouj, J. Galmiche, J. Abrams, A. Rastogi *et al.*, "Real-time increased detection of neoplastic tissue in barrett's esophagus with probe-based confocal laser endomicroscopy: final results of an international multicenter, prospective, randomized, controlled trial," *Gastrointestinal endoscopy*, vol. 74, no. 3, pp. 465–472, 2011.

[8] B. Rosa, B. Herman, J. Szewczyk, B. Gayet, and G. Morel, "Laparoscopic optical biopsies: in vivo robotized mosaicing with probe-based confocal endomicroscopy," in *Intelligent Robots and Systems (IROS), 2011 IEEE/RSJ International Conference on*. IEEE, 2011, pp. 1339–1345.

[9] W. Latt, T. Chang, A. Di Marco, P. Pratt, K. Kwok, J. Clark, and G. Yang, "A hand-held instrument for in vivo probe-based confocal laser endomicroscopy during minimally invasive surgery," in *Intelligent Robots and Systems (IROS), 2012 IEEE/RSJ International Conference on*. IEEE, 2012, pp. 1982–1987.

[10] T. Vercauteren, A. Perchant, G. Malandain, X. Pennec, and N. Ayache, "Robust mosaicing with correction of motion distortions and tissue deformations for in vivo fibered microscopy," *Medical Image Analysis*, vol. 10, no. 5, pp. 673–692, Oct. 2006.

[11] K. E. Loewke, D. B. Camarillo, W. Piyawattanametha, M. J. Mandella, C. H. Contag, S. Thrun, and J. K. Salisbury, "In vivo micro-image mosaicing," *IEEE Trans. Biomed. Eng.*, vol. 58, no. 1, pp. 159–171, Jan. 2011.

[12] M. Erden, B. Rosa, J. Szewczyk, and G. Morel, "Mechanical design of a distal scanner for confocal microlaparoscope: a conic solution," in *IEEE International Conference on Robotics and Automation (ICRA)*, 2013, to appear.

[13] ——, "Understanding soft tissue behavior for application to microlaparoscopic surface scan," *IEEE Transactions on Biomedical Engineering*, vol. 60, no. 4, pp. 1059 – 1068, 2013.

[14] J. P. Lewis, "Fast template matching," in *Proceedings of the International Conference on Vision Interface (VI'95)*, 1995, pp. 120–123.

[15] B. Rosa, M. Erden, T. Vercauteren, B. Herman, J. Szewczyk, and G. Morel, "Building large mosaics of confocal endomicroscopic images using visual servoing," *IEEE Transactions on Biomedical Engineering*, vol. 60, no. 4, pp. 1041 – 1049, 2013.